



Research article

ICG fluorescence imaging technology in laparoscopic liver resection for primary liver cancer: A meta-analysis

Pan Lu, Wei Zhang, Long Chen, Wentao Li and Xinyi Liu*

Department of Hepatobiliary Surgery, Jianyang People's Hospital, Jianyang, Sichuan, China

* **Correspondence:** Email: 2018020199@stu.cdut.edu.cn.

Abstract: *Objective:* To study the value of ICG molecular fluorescence imaging in laparoscopic hepatectomy for PLC. *Methods:* CNKI, WD, VIP.com, PM, CL and WOS databases were selected to search for literature on precise and traditional hepatectomy for the treatment of PLC. *Results:* A total of 33 articles were used, including 3927 patients, 2102 in precision and 1885 in traditional. Meta showed that the operation time of precision was longer, while IBV, HS, PLFI, ALT, TBil, ALB, PCR, PROSIM, RMR and 1-year SR had advantages. *Conclusion:* Hepatectomy with the concept of PS is a safe and effective method of PLC that can reduce the amount of IB, reduce surgery, reduce PC and improve prognosis and quality of life.

Keywords: ICG indocyanine green; fluorescence imaging; precision liver resection; primary liver cancer; concept of precision surgery; meta-analysis

1. Introduction

Primary Liver Cancer (PLC) is one of the most common malignant tumors of the digestive system. Its incidence and fatality rates are as high as those of the top three [1,2]. It was found that men have a higher risk of liver cancer than women. The male-to-female ratio of the global incidence of liver cancer is 2.8:1. Among the pathological types of PLC, HCC constitutes the most common, accounting for approximately 85–90%, and the rest are koniocellular carcinoma and mixed hepatocellular carcinoma. PLC treatment is complex, and patients must choose a reasonable treatment plan according to different tumor stages. Liver resection is still the most critical method for long-term survival in patients with a good liver reserve. Complete resection of the tumor tissue at an early stage improves the prognosis of

patients and is expected to achieve a curative effect.

[3,4] Laparoscopic hepatectomy has been increasingly used to treat liver tumors. Since hepatectomy with laparoscopy, the number of reports on treating various tumors has increased. One of the challenges faced by surgeons performing laparoscopic hepatectomy is that preoperative imaging studies may miss lesions in indeterminate anatomical regions [5,6]. These lesions are difficult to treat because of the limited visibility of laparoscopy and the inability to palpate, thus losing the most intuitive feeling of traditional surgery on lesions. When it comes to the removal of malignant tumor, the primary goal is to eliminate the tumor while ensuring a tumor-free margin. Additionally, it is important to retain a sufficient volume of liver tissue to ensure optimal function. These basic principles are essential in the field of oncology and guide medical professionals in their approach to treating these types of tumors. Therefore, it is very important to completely find and analyze the relationship between the tumor on the liver and the location of the intrahepatic duct, which will help reduce the postoperative recurrence rate [7,8]. It is challenging for surgeons to accurately mark tumor resection lines when performing surgery. To overcome this problem, new imaging techniques are needed for precise laparoscopic hepatectomy. ICG fluorescence imaging technology can make up for the shortcomings of existing methods and provide a feasible way to accurately define the edge of liver cancer and accurately remove tumors [9,10]. Through the role of ICG, the location and boundary of liver cancer can be displayed in real time during the operation, which is helpful for surgeons to adjust the resection line of the liver in time and remove tumors efficiently and accurately. With wide application of this technology, the resection rate of tumors and satellite lesions will be greatly improved, and R0 resection of liver parenchyma and maximum preservation will be realized.

Indocyanine green is a unique heptacyanine dye reagent that can be used in the human body, and its function and significance are significant. After being injected into the human body through superficial peripheral blood vessels, 98%–99% of ICG is bound to serum proteins and is taken up by hepatocytes under the combined action of the organic anion transporter 1B3 and the sodium ion-taurocholic acid co-transporter [6]. It is excreted into the biliary tract through the multidrug-resistance-related protein 2 vector system expressed on capillary bile ducts. This process does not involve lymphatic return and does not participate in enterohepatic circulation. In healthy liver tissue, it only takes a few hours for ICG to be completely excreted into the biliary tract and finally excreted through the intestinal tract. When liver tumors or other pathological changes occur, ICG cannot be excreted through bile, so it accumulates in diseased tissue and the phenomenon of developing can occur. Because ICG is excreted through the biliary tract, it can also be used for the detection of intraoperative bile leakage. ICG is also a near-infrared fluorescent dye, which can be excited by external light with a wavelength of 750–810 nm and emit near-infrared light that cannot be seen by the naked eye with a wavelength of about 850 nm, but through a special imaging system (PDE) can be displayed on a display device after receiving. Due to the weak penetration of near-infrared light with a wavelength of 850 nm, lesions with a depth greater than 10 mm cannot be visualised in PDE [6–8]. Moreover, due to its special chemical structure, sterile water for injection becomes the first solvent for ICG rather than normal saline. The salt solution accelerates the aggregation of ICG molecules. At present, ICG fluorescence imaging technology has been accepted by surgeons, and reports on the use of ICG for laparoscopic liver resection are gradually increasing. [11,12] reported that ICG could be used for intraoperative staining of liver segments [13,14]. To determine the margin of liver resection during laparoscopic surgery, fluorescence properties of ICG were used [15,16]. Reported that preoperative veins Injection of ICG can identify primary and secondary liver malignancies. [17,18] accumulated a lot of experience

in the use of ICG in laparoscopic liver resection, which has led to continuous improvement and perfection of this technology. ICG has made great contributions to the differentiation of small tumors, boundary division, liver segment definition and bile leakage. The way, time, and dosage of ICG injection for patients are different according to different purposes. At present, the time and dosage of preoperative administration are still in the exploration stage. With the proposal of the “concept of PH” [19,20], imaging technology of ICG in laparoscopic hepatectomy is also developing with time. Compared with conventional laparoscopic surgery, the use of ICG has greatly improved the tumor resection rate and prognosis of patients.

The main content of this study is to consult relevant literature on the comparison between precision hepatectomy and traditional hepatectomy, make a comprehensive comparison between the two treatment methods with the method of meta-analysis, and draw conclusions.

2. Materials and methods

2.1. Literature collection

In this study, databases of PubMed, Cochrane Library (CL), Web of Science (WOS), China National Knowledge Infrastructure Database (CNKI), Wanfang and Vindex Protein domain (VIP) were searched for literature published from January 1, 2009 to November 1, 2021, using title search, Chinese search terms for: PH, AH, traditional hepatectomy, traditional hepatectomy, PLC; English search terms are peri-hilar cholangiocarcinoma (PH), platelet-to-lymphocyte ratio (PLR), Aryl hydrocarbon (AH) receptor, Primary Liver Cancer (PLC), hepatocellular carcinoma (HC), Liver cancer (LC).

2.2. Inclusion criteria

1) The included literature was from 2009.1.1 to 2021.11.1, and the postoperative pathology of all cases met diagnostic criteria for PLC.

2) There is a comparison between precision and tradition in intervention and treatment measures for PLC.

3) The experimental design is a randomized controlled trial or a clinically controlled trial.

4) Observation indicators at least include operation time, intraoperative blood loss, average hospital stays, postoperative AST, alanine transaminase (ALT) and total bilirubin (TbIL). One of the indicators is the incidence of serum albumin (ALB) complications, the positive rate of specimen margins, the recurrence and metastasis rate and the 1-year survival rate after surgery.

5) Good liver function indicators, Child score A/B, or grade C converted to grade B after medical treatment; no major underlying disease; cannot tolerate surgery.

6) Diagnostic Criteria: To diagnose PLC, imaging techniques such as CT, MRI and ultrasound are used to confirm the presence of characteristic findings consistent with liver cancer, such as arterial enhancement and washout in the venous or delayed phases. Additionally, the diagnosis can be confirmed by histopathological examination of liver tissue obtained through biopsy or surgical resection, which may include the identification of hepatocellular carcinoma (HCC) or other primary liver malignancies.

2.3. Exclusion criteria

- 1) The literature is not a controlled study but only a case report or review.
- 2) The literature scores are low, the quality is poor, the information is limited and there is no literature involving observation indicators.
- 3) Documents whose data cannot be obtained by computer
- 4) If it is duplicate data published by the same centre or literature published after expanding the sample size, literature with higher quality will be selected.

2.4. Clinical observation indicators

Including operation time, total intraoperative blood loss, average hospital stays and postoperative liver function indexes, including AST, ALT, TBI_L, ALB, incidence of complications, positive rate of specimen margins, rate of recurrence and metastasis and 1-year survival rate after surgery.

2.5. Quality evaluation

The evaluation criteria included: ① random distribution; ② Whether there is a distribution plan; ③ Whether blind method is used; ④ Whether data results are lost; ⑤ Whether selected experimental results are reported; ⑥ Whether there are other sources of bias. Different researchers evaluate quality of selected literature, exchange different opinions and seek quality evaluation results of third party.

3. Results

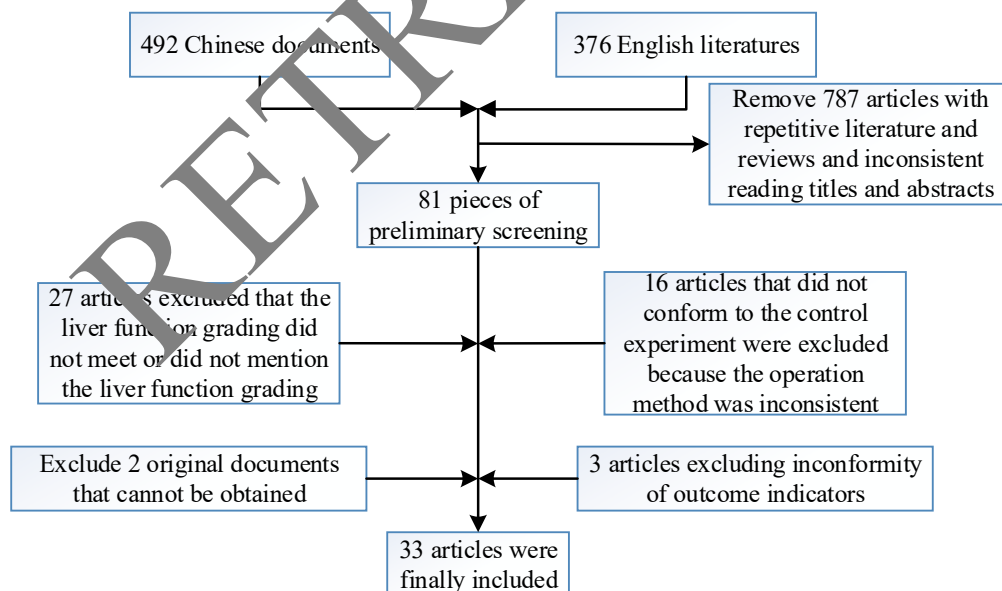


Figure 1. Pieces of preliminary screening.

In this study, literatures published from January 1, 2009, to November 1, 2021, were retrieved. The included literatures were retrieved by title and imported into NoteExpress software. A total of 868

related literatures were collected, including 492 Chinese literatures and 376 English literatures. Through inclusion criteria, exclusion criteria, careful reading of full text and screening strategies, Finally, 33 high-quality literatures were obtained, including 27 Chinese literatures and 6 English literatures, totaling 3987 cases, 2102 in precision and 1885 in traditional. Figure 1 below shows flow chart made according to established screening strategy, and Table 1 shows general situation of included literature.

Table 1. Basic characteristics of included literature.

Serial No.	Author and year	Total number of cases (n)	Number of cases (n)		Liver function child Classification
			Precision	Legacy Group	
1	Wang Xintuan 2018	72	36	36	A/B
2	Xu Jiwei 2016	70	35	35	A/B
3	Wang Zhu 2015	80	40	40	A/B
4	Huang Hai 2014	100	50	50	A/B
5	Liu Jie 2017	62	31	31	A/B
6	Li Liuzheng 2019	202	101	101	A/B
7	Li Bo 2019	220	110	110	A/B
8	Yang Feilong 2019	98	49	49	A/B
9	Wu Zhaofeng 2018	90	45	45	A/B
10	Li Xiaoming 2017	98	49	49	A/B
11	Ni Peng 2017	40	20	20	A/B
12	Liu Yifei 2017	88	44	44	A/B
13	Zhong Tiegang 2015	68	34	33	A/B
14	Zhang Zhihua 2014	92	46	46	A/B
15	Luo Hanchuan 2014	75	42	33	A/B
16	Liu Jing 2014	100	50	50	A/B
17	Zhang Shubin 2019	108	54	54	A/B
18	Fang Chao 2019	100	50	50	A/B
19	Qiu Yudong 2013	60	30	30	A/B
20	Yangke 2014	80	45	35	A/B
21	Song Tianqiang 2021	86	42	44	A/B
22	Jiang Xu 2016	64	32	32	A/B
23	Chen Ya 2016	72	47	25	A/B
24	Wang Zhongju 2018	64	34	30	A/B
25	Zhang Song 2015	207	158	49	A/B
26	Kaibori2017	710	355	355	A/B
27	Okamura2014	236	97	97	A/B
28	Sasaki2013	87	57	57	A/B
29	Eltawil 2010	53	25	25	A/B
30	Yamamoto 2017	173	48	48	A/B
31	Tomimaru 2012	92	62	62	A/B
32	Cai Lijun 2015	120	60	60	A/B
33	Zhang Lixian 2018	120	60	60	A/B

Table 2. Comparison of OT between precision and traditional.

Study or Subgroup	Precision			General			Weight	Mean Difference IV, Random.95%CI
	Mean	SD	Total	Mean	SD	Total		
Tomimaru 2012	253	78	30	213	59	62	3.4%	40.02 [8.44,71.56]
Qiu Yudong 2013	291	91	30	282	93	30	2.6%	9.02 [-37.54,55.55]
Wu Zhao Feng 2018	81.4	12.3	45	96.6	11.3	45	4.7%	-15.22 [-20.06,-10.34]
Ni Peng 2017	168.4	21.8	20	92.2	14.6	20	4.5%	76.22 [64.84,87.56]
Liu Yifei 2017	97.4	9.9	44	78.4	6.6	44	4.7%	19.02 [15.52,22.52]
Liu Jie 2017	168	24	31	90	18	31	4.5%	78.02 [67.46,88.58]
Jiang Xu 2018	173.6	34.4	32	103.6	29.6	32	4.3%	69.62 [53.99,85.25]
Zhang Zhihua 2014	97.36	9.68	46	78.18	6.96	46	4.7%	19.17 [15.76,22.64]
Zhang Song 2015	153.5	38.5	158	190.6	55.4	49	4.3%	-36.72 [-53.35,-20.05]
Zhang Shubin 2019	190.56	23.77	54	161.04	16.63	54	4.5%	29.54 [21.77,37.27]
Zhang Lixian 2018	236.6	54.43	60	181.66	45.24	60	4.2%	54.78 [36.88,72.68]
Xu Jicheng 2016	102.6	23.3	35	98.5	21.5	35	4.5%	4.12 [-6.33,14.53]
Fang Chao 2019	73.54	4.83	50	89.44	2.13	50	4.7%	-15.92 [-19.53,-12.27]
Li Xiaoming 2017	260.57	26.35	49	182.66	18.56	49	4.6%	77.87 [68.84,86.86]
Li Liuzheng 2019	331.3	42.5	101	318.3	52.3	101	4.4%	13.32 [0.13,26.47]
Li Bo 2019	329.67	50.14	110	301.76	30.45	110	4.5%	27.93 [16.93,38.88]
Yangke 2014	205.2	11.6	45	164.5	7.6	35	4.7%	41.12 [36.86,45.34]
Yang Feilong 2019	102.36	15.45	49	98.28	15.55	49	4.9%	5.08 [-1.02,11.14]
Wang Zhongju 2018	366.13	50.44	34	306.48	51.36	3060	3.6%	61.67 [36.67,86.67]
Wang Xintuan 2018	103.6	23.3	36	98.8	22.7	365	4.6%	4.92 [-5.65,15.45]
Wang Zhu 2015	99.3	8.23	40	75.03	6.44	40	4.6%	24.47 [21.26,27.76]
Cai Lijun 2015	240.8	60.5	60	172.3	41.6	60	4.4%	68.12 [49.57,86.63]
Huang Hai 2014	254.6	29.9	50	174.4	41.7	50	4.2%	80.21 [65.96,94.43]
Total (95% CI)			1209			1118	100.0%	31.75 [20.82,42.76]

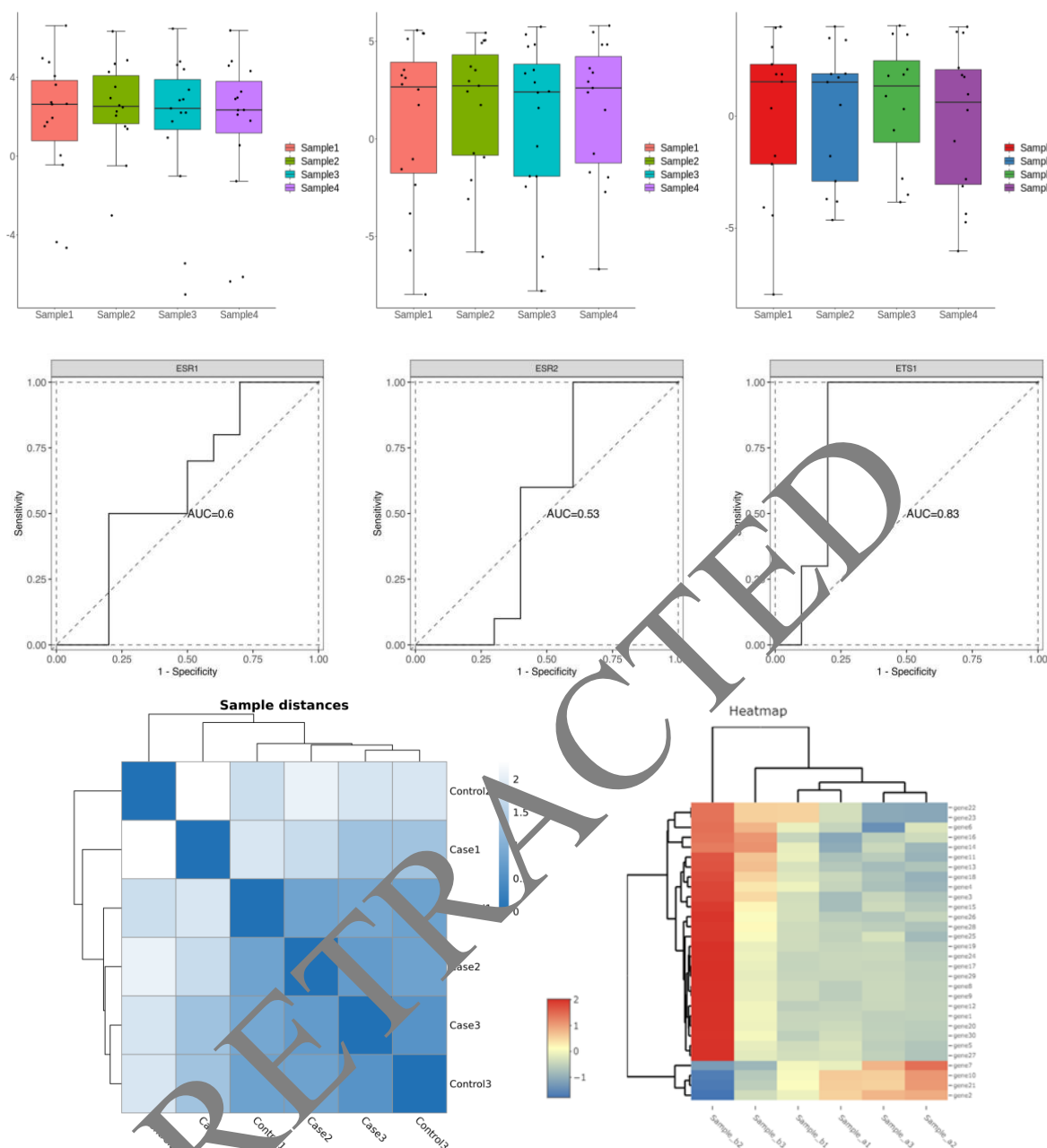


Figure 2. Comparison of the operative time (OT) between two approaches: precision and traditional, in the context of laparoscopic liver resection for primary liver cancer (PLC).

There are 23 articles included to compare operation time. Among the included cases, there are 1209 cases in precision and 1118 cases in traditional. There is heterogeneity between outcome indicators, so random effect model. The MD is 31.77, 95% CI (20.80,42.74) in Figure 2 and Table 2. The combined effect amount test result $Z = 5.68$, $P < 0.0001$, Therefore, operation time was significant. The operation time of precision was longer than that of traditional.

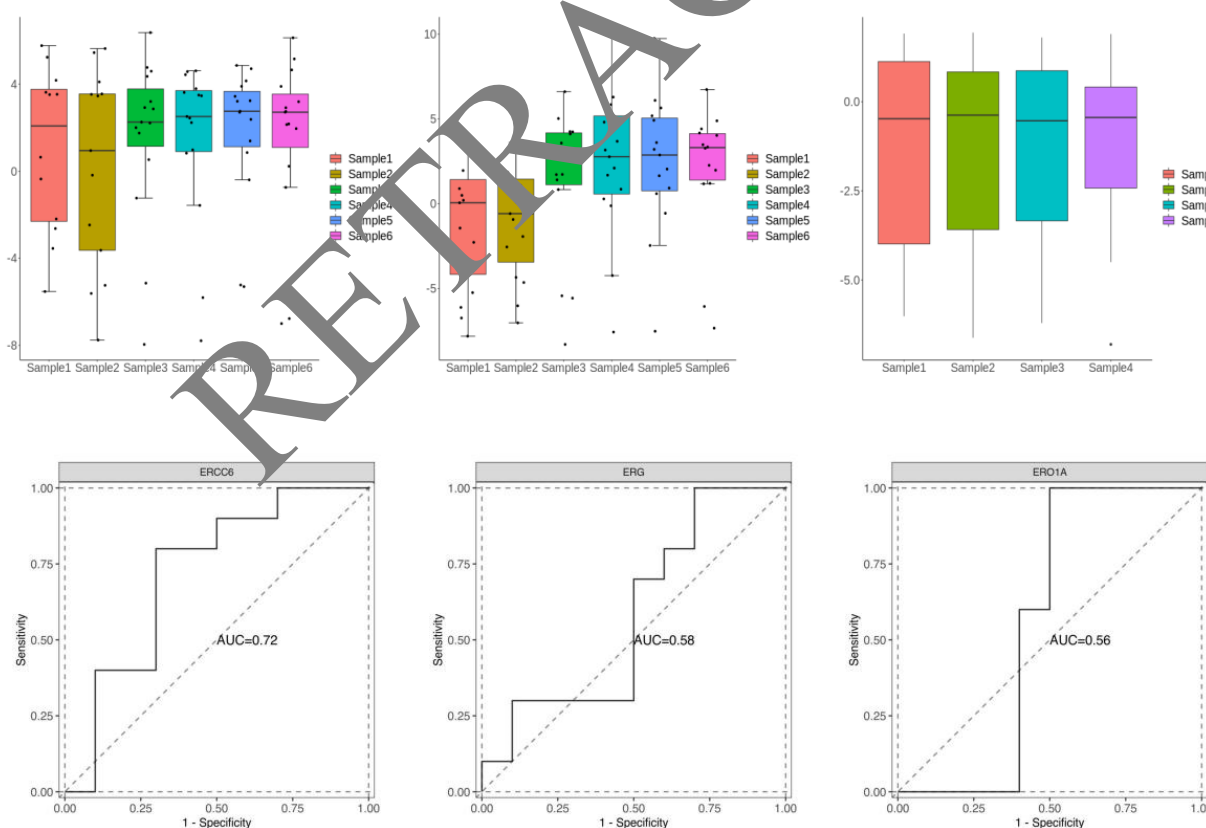
Table 3. Comparison of IBL between precision and traditional.

Study or Subgroup	Precision			General			Weight	Mean Difference IV, Random.95%CI
	Mean	SD	Total	Mean	SD	Total		
Tomimaru 2012	1.113	809	30	756	702	62	0.8%	356.00 [17.86,694.14]
Qiu Yudong 2013	638	264	30	588	233	30	2.6%	50.00 [76.00,176.00]
Wu Zhao Feng 2018	234.6	26.6	45	378.8	21.5	45	4.3%	-143.80 [-153.78,-133.82]
Ni Peng 2017	431.54	124.55	20	764.55	114.66	20	3.5%	-333.05 [-407.24,-258.86]
Liu Yifei 2017	220	26.3	44	386.7	22.6	44	4.3%	-166.50 [176.83,-156.17]
Liu Jie 2017	359.4	143.1	31	746.3	237.8	31	3.1%	-386.90 [-484.56,-289.24]
Liu Jing 2014	710.26	39.26	50	871.24	45.93	50	4.2%	-160.54 [-177.69,-144.19]
Jiang Xu 2018	437.66	179.44	32	762.88	249.01	32	2.9%	-325.17 [-431.53,-218.85]
Song Tianqiang 2021	320	315	42	613	526	44	1.8%	-222.00 [-475.29,-110.71]
Zhang Zhihua 2014	221.25	27.97	46	382.54	22.64	46	4.3%	-161.33 [-171.73,-150.93]
Zhang Song 2015	209.7	196.4	158	330.3	137.6	49	3.9%	-120.20 [169.44,-70.96]
Zhang Shubin 2019	204.97	169.68	54	298.65	212.66	54	3.5%	-93.69 [166.26,-21.12]
Zhang Lixian 2018	542.03	70.94	60	696.95	88.14	60	4.1%	-154.92 [-183.54,-126.30]
Xu Jiwei 2016	214.4	37.7	35	379.5	45.2	35	4.2%	-164.70 [-184.13,-145.27]
Fang Chao 2019	89.7	6.25	50	122.15	10.92	50	4.3%	-32.33 [-35.82,-28.84]
Li Xiaoming 2017	490.67	50.75	49	657.77	67.82	49	4.2%	-167.10 [-190.81,-143.39]
Li Liuzheng 2019	525.7	64.2	101	709.7	61.1	101	4.2%	-204.30 [-221.58,-187.02]
Li Bo 2019	509.76	32.17	110	694.86	44.99	110	4.3%	-185.14 [-195.47,-174.81]
Yangke 2014	621.3	221.5	45	942.3	353.5	35	2.5%	-321.00 [-454.89,-187.11]
Yang Feilong 2019	201.64	20.63	49	365.26	26.76	49	4.3%	-163.66 [-173.11,-154.21]
Wang Zhongju 2018	556.88	80.51	34	785.44	85.78	30	4.0%	-228.60 [-269.52,-187.68]
Wang Xintuan 2018	213.3	32.5	36	386.4	34.6	36	4.2%	-172.70 [-188.21,-157.19]
Wang Zhu 2015	220.53	25.25	40	385.06	35.35	40	4.3%	-164.54 [-178.05,-151.07]

Continued on next page

Study or Subgroup	Precision			General			Weight	Mean Difference IV, Random.95%CI
	Mean	SD	Total	Mean	SD	Total		
Wang Zhu 2015	220.53	25.25	40	385.06	35.35	40	4.3%	-164.54 [-178.05,-151.07]
Luo Hanchuan 2014	61.4	435	42	1.323	557	33	1.3%	-713.01 [-944.11,-418.86]
Cai Lijun 2015	558.5	90.4	60	726.5	88.8	60	4.1%	-168.42 [-200.47,-136.34]
Zhong Tie 2015	150	30	36	270	20	33	4.3%	-120.01 [-132.08,-136.34]
Chen Ya 2018	320	145	47	313	246	25	2.9%	7.02 [-97.97,111.97]
Huang Hai 2014	487.2	119.6	50	654	192.3	50	3.7%	-166.92 [-229.57,-104.23]
Total (95% CI)			1425			1303	100.0%	-173.52 [-205.82,-141.22]

There are 28 articles included to compare amount of intraoperative bleeding. Among the included cases, there are 1425 cases in precision and 1303 cases in traditional. There is heterogeneity between outcome indicators. Therefore, random effect model is used for combined analysis. The combined effect amount MD is -173.50, 95% CI (-205.80,-141.21). See Figure 3 and Table 3. The combined effect amount test results $Z = 10.53$, $P < 0.0001$. Therefore intraoperative bleeding was significant. The bleeding in precision was less than that in traditional.



Continued on next page

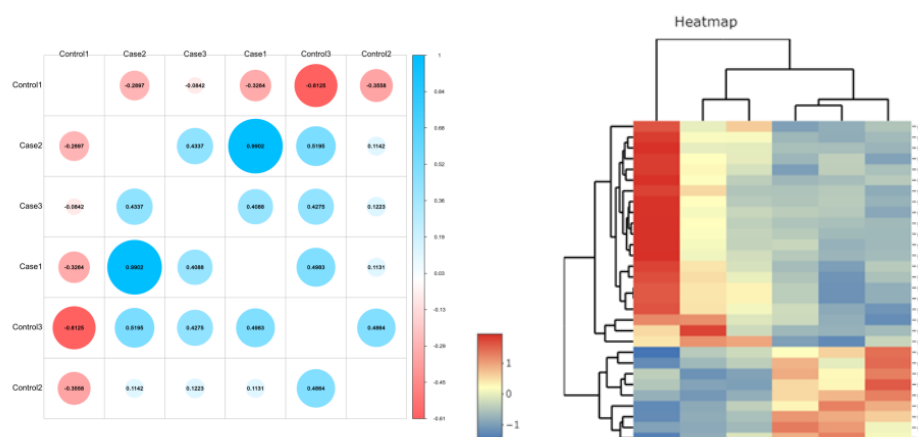


Figure 3. Comparison of the average hospital stay (AHS) between two approaches: precision and traditional, in the context of laparoscopic liver resection for primary liver cancer (PLC).

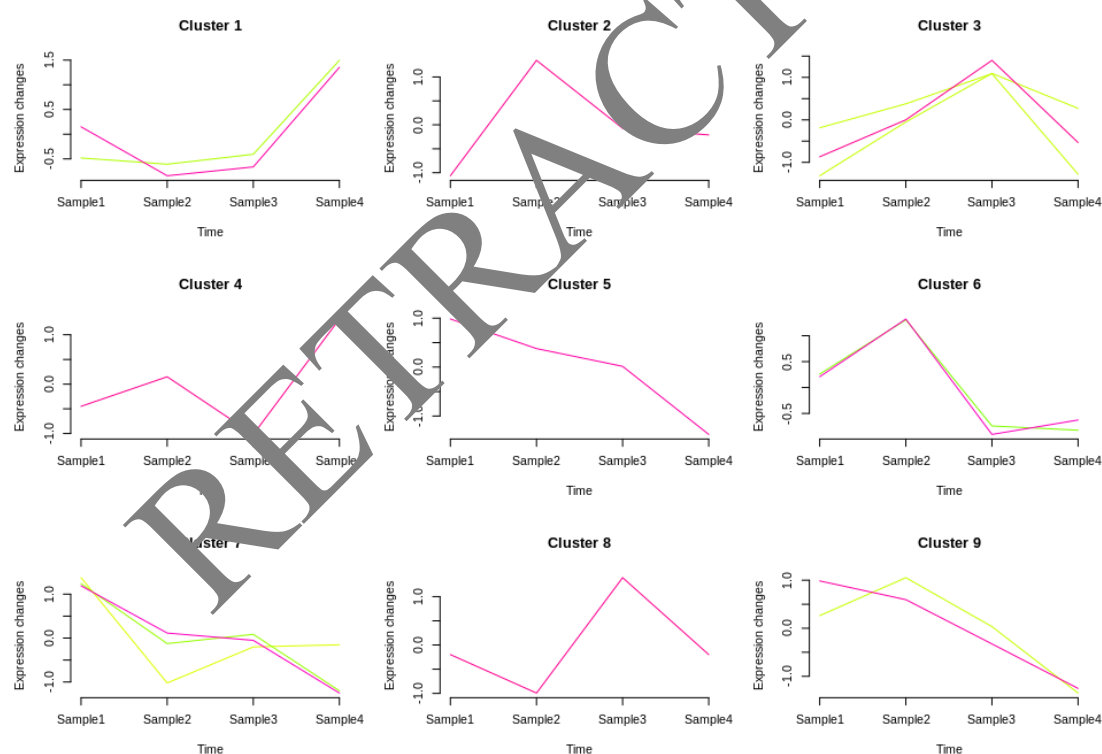


Figure 4 Comparison of the average hospital stay (AHS) between two approaches: precision and traditional, in the context of laparoscopic liver resection for primary liver cancer (PLC).

Table 4. Comparison of AHS between precision and traditional.

Study or Subgroup	Precision			General			Weight	Mean Difference IV, Random.95%CI
	Events		Total	Events		Total		
Tomimaru 2012	20	13	30	19	10	62	1.9%	1.00 [-4.28,6.28]
Wu Zhao Feng 2018	7.7	1.1	45	12.8	2.9	45	5.1%	-4.70 [-5.56,-3.84]
Liu Yifei 2017	8.4	0.6	44	12.4	1.7	44	5.2%	-4.00 [-4.61,-3.39]
Jiang Xu 2018	9.33	2.05	32	13.74	3.54	32	4.7%	-4.37 [-5.79,-2.95]
Zhang Zhihua 2014	8.35	0.7	46	12.16	1.92	46	5.2%	-3.81 [-4.41,-3.21]
Zhang Song 2015	6.7	2.3	158	10.6	4	49	4.9%	-3.90 [-5.07,-2.73]
Zhang Shubin 2019	7.83	2.24	54	8.93	3.35	54	4.9%	-0.14 [-2.22,-0.06]
Zhang Lixian 2018	15.15	2.04	60	17.34	2.27	60	5.1%	-2.16 [-2.93,-1.39]
Xu Jiwei 2016	8.7	2.3	35	12.6	3.6	35	4.7%	-3.90 [-5.25,-2.55]
Fang Chao 2019	9.77	1.44	50	12.68	4.23	50	4.8%	-2.90 [-4.14,-1.66]
Li Xiaoming 2017	14.97	1.55	49	17.44	2.44	49	5.1%	-2.44 [-3.25,-1.63]
Li Liuzheng 2019	16.3	3.6	101	21.3	4.3	101	5.0%	-8.40 [-9.44,-7.36]
Li Bo 2019	18.18	4.66	110	23.05	6.17	110	4.7%	-4.88 [-6.33,-3.43]
Yangke 2014	11.8	3.4	45	17.8	4.3	35	4.5%	-6.00 [-7.65,-4.35]
Yang Feilong 2019	8.18	2.97	49	12.35	3.42	49	4.8%	-4.17 [-5.44,-2.90]
Wang Zhongju 2018	15.44	2.4	34	24.43	3.7	30	4.5%	-8.99 [-10.57,-7.41]
Wang Xintuan 2018	8.5	2.5	36	12.6	13.5	3	2.2%	-3.90 [-8.44,-0.64]
Wang Zhu 2015	8.5	0.7	40	12.6	1.6	40	5.2%	-4.00 [-4.54,-3.46]
Cai Lijun 2015	12.2	3.4	60	24.4	7.7	60	4.1%	-12.50 [-14.56,-10.44]
Zhong Tiegang 2015	11	4	35	23	7	33	3.5%	-12.00 [-14.73,-9.27]
Chen Ya 2018	12.5	2.5	47	12.4	2.6	25	4.8%	-0.30 [-1.50,0.90]
Huang Hai 2014	14.1	1.3	50	17.3	2.5	50	5.1%	-2.80 [-3.55,-2.05]
Total (95% CI)			1210			1095	100.0%	-4.55 [-5.44,-3.66]

The average length of stay was compared in 22 included literatures. The number of included cases was 1210 in precision and 1095 in traditional. There are homogeneity between outcome indicators. The MD was -4.55, 95% CI (-5.44,-3.66) in Figure 4 and Table 4. The combined effect amount test results $Z = 9.99$, $P < 0.0001$. Therefore average hospital stay was significant, and average hospital stay of precision was shorter than that of traditional.

Table 5. Comparison of PCR between precision and traditional.

Study or Subgroup	Precision		General		Weight	Odds Ratio M-H. Fixed, 95%CI
	Events	Total	Events	Total		
Sasaki 2013	3	30	5	57	1.1%	1.15 [0.25,5.22]
Tomimaru 2012	21	30	52	62	3.5%	0.43 [0.14,1.25]
Yamamoto 2017	20	125	7	48	2.9%	1.14 [0.42,2.86]
Qiu Yudong 2013	7	30	15	30	4.0%	0.32 [0.12,0.93]
Wu Zhaofeng 2018	2	45	10	45	3.3%	0.14 [0.05,0.77]
Liu Yifei 2017	2	44	7	44	2.3%	0.23 [0.03,1.27]
Liu Jie 2017	2	31	14	31	4.5%	0.06 [0.01,0.42]
Liu Jing 2014	4	50	14	50	4.5%	0.22 [0.07,0.75]
Jiang Xu 2018	1	32	5	32	1.7%	0.15 [0.04,1.56]
Song Tianqiang 2021	3	42	9	44	2.8%	0.32 [0.05,1.17]
Zhang Zhihua 2014	4	46	7	46	2.2%	0.51 [0.16,1.95]
Zhang Song 2015	19	158	15	49	7.0%	0.33 [0.13,1.93]
Zhang Lixian 2018	7	60	16	60	2.9%	0.34 [0.16,0.95]
Xu Jiwei 2016	2	35	8	35	2.6%	0.22 [0.05,1.06]
Fang Chao 2019	1	50	8	50	2.7%	0.13 [0.02,0.87]
Li Xiaoming 2017	3	49	12	49	3.9%	0.22 [0.04,0.75]
Li Liuzheng 2019	12	10	26	101	7.9%	0.37 [0.16,0.84]
Li Bo 2019	25	110	35	110	10.4%	0.55 [0.32,0.99]
Yangke 2014	3	45	16	35	5.8%	0.06 [0.01,0.31]
Wang Zhongju 2018	10	34	17	30	4.4%	0.34 [0.13,0.88]
Wang Zhu 2015	3	40	6	40	1.9%	0.44 [0.13,1.97]
Luo Hanchuan 2014	4	42	9	33	3.2%	0.26 [0.06,1.03]
Cai Lijun 2015	6	63	20	60	6.2%	0.23 [0.06,0.62]
Chen Ya 2018	10	47	6	25	2.1%	0.88 [0.25,2.73]
Huang Hai 2014	5	50	13	50	4.0%	0.33 [0.12,0.99]
Total (95% CI)		1386		1216	100.0%	0.35 [0.27,0.44]
Total events	170		356			

The incidence of complications was compared in 25 included literatures. There were 1386 cases in precision and 1216 cases in traditional. There are homogeneity between outcome indicators. The OR was 0.34, 95% CI (0.28, 0.43) in Figure 5 and Table 5. The combined effect amount was $Z = 9.67$, $P < 0.0001$. Therefore, incidence of complications was significant, and incidence of postoperative complications was low in precision.

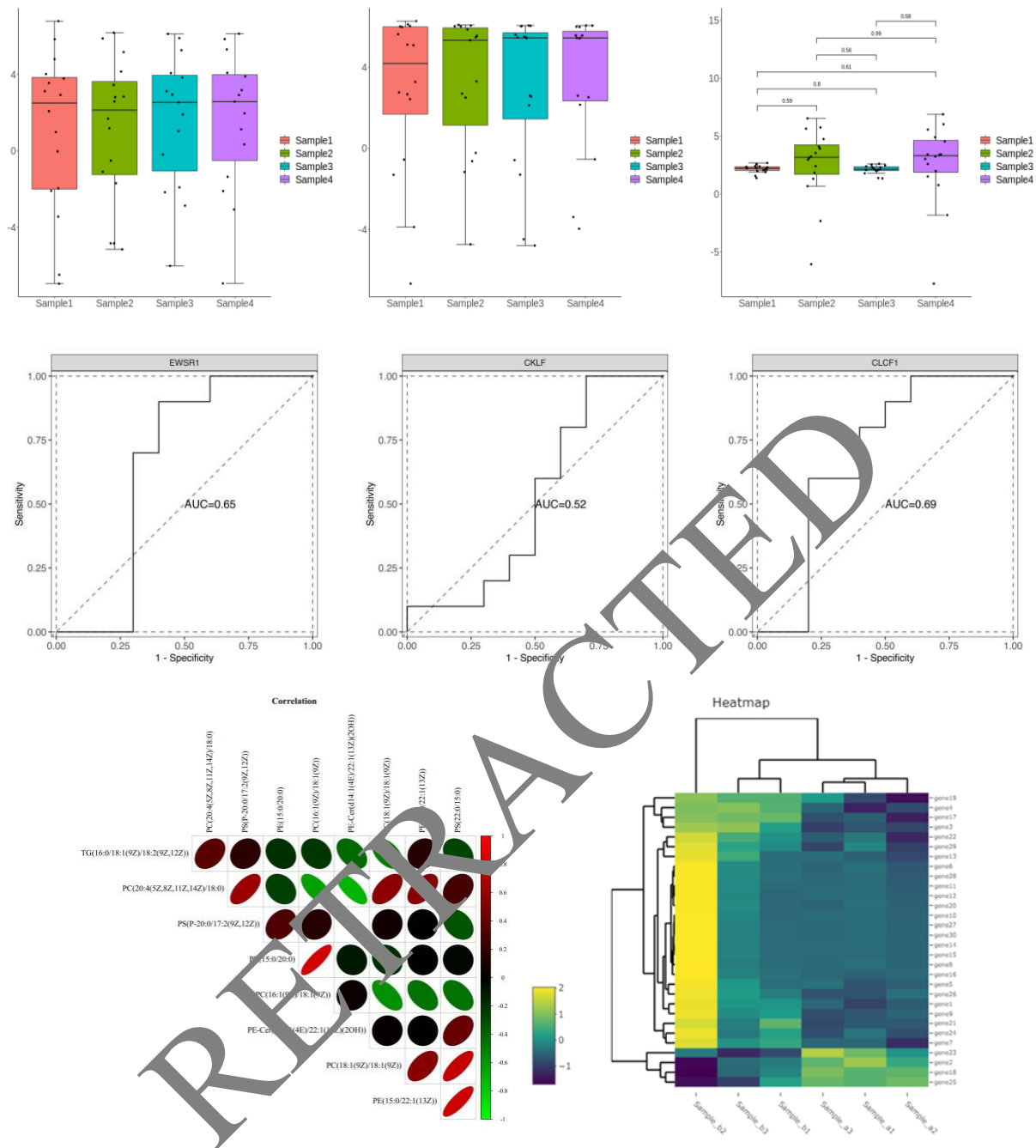
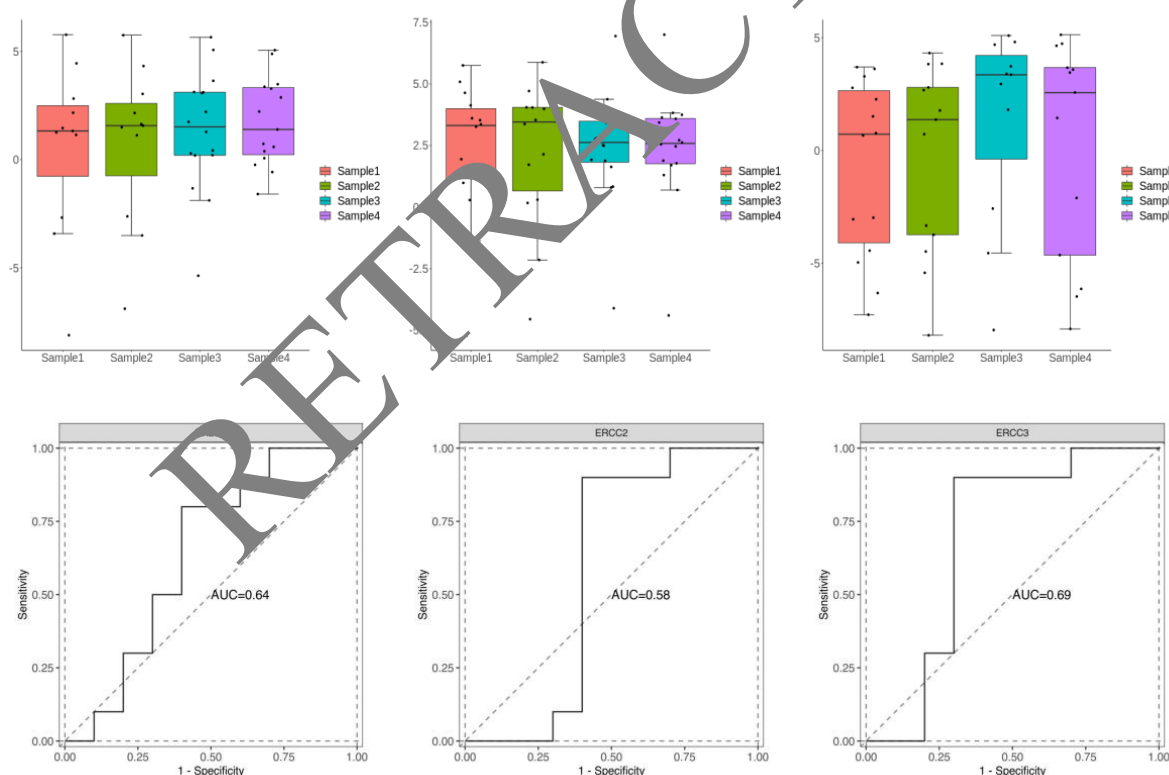


Figure 5. Comparison of the PCR between two approaches: precision and traditional, in the context of laparoscopic liver resection for primary liver cancer (PLC).

Table 6. Comparison of positive rate of surgical margins.

Study or Subgroup	Precision		General		Weight	Odds Ratio M-H. Fixed, 95%CI
	Events	Total	Events	Total		
Kaibori 2017	5	355	17	322	25.9%	0.25 [0.07,0.72]
Okamura 2014	5	139	6	97	10.0%	0.56 [0.15,1.92]
Li Xiaoming 2017	4	49	14	49	18.9%	0.23 [0.06,0.74]
Li Liuzheng 2019	8	101	18	101	24.4%	0.42 [0.15,0.95]
Luo Youchuan 2014	3	42	7	33	10.7%	0.27 [0.06,1.23]
Huang Hai 2014	1	50	7	50	10.1%	0.14 [0.02,1.05]
Total (95% CI)		736		652	100.0%	0.31 [0.18,0.48]
Total events	26		69			

There are 6 articles included to compare positive rate of specimen incisional margin. There are 736 cases in precision and 652 cases in traditional. There are homogeneity between outcome indicators. The amount OR is 0.31, 95% CI (0.19, 0.49). See Figure 6 and Table 6. The combined effect is $Z = 4.92$, $P < 0.0001$. Therefore, complications is significant, and positive rate of incisional margin in precision was low.



Continued on next page

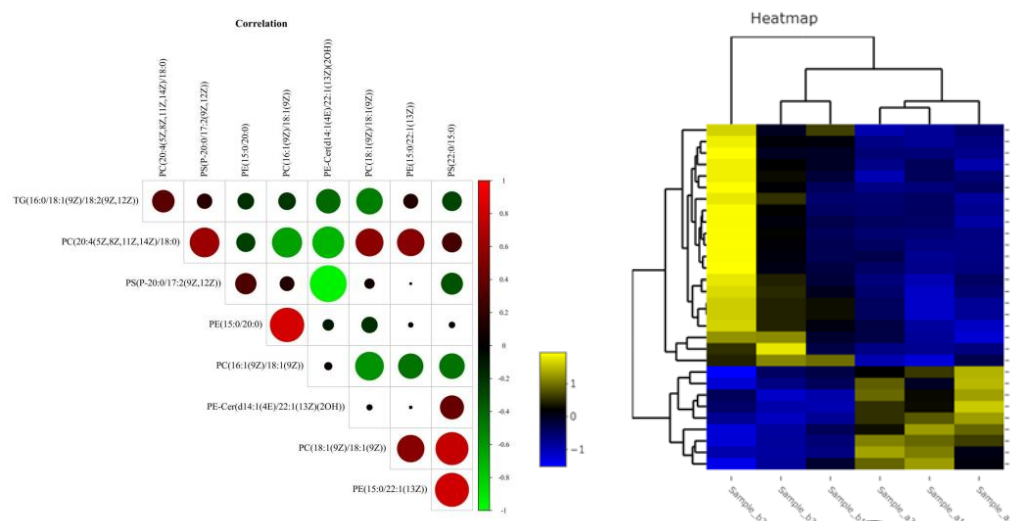


Figure 6. Comparison of the positive rate of surgical margins between different approaches, specifically the use of ICG fluorescence imaging technology and traditional methods.

There are 12 articles included to compare recurrence and metastasis rate. There are 785 cases in precision and 815 cases in traditional. There are homogeneity between outcome indicators. The OR is 0.62, 95% CI (0.50, 0.78). See Figure 7 and Table 7. The combined effect is $Z = 4.17$, $P < 0.0001$. Therefore, recurrence and metastasis rates are significant, and recurrence and metastasis rate in precision was low.

Table 7. Comparison of RM rates between precision and traditional.

Study or Subgroup	Precision		General		Weight	Odds Ratio M-H. Fixed, 95%CI
	Events	Total	Events	Total		
KM. Eltawil 2010	10	28	25	28	3.4%	0.82 [0.25,2.56]
Kaibori 2017	191	355	206	355	47.5%	0.86 [0.65,1.11]
Tomimaru 2012	12	30	32	62	6.3%	0.65 [0.24,1.53]
Qiu Yudong 2013	3	30	5	30	2.2%	0.54 [0.14,2.55]
Wu Zhaofeng 2016	1	45	8	45	3.9%	0.13 [0.02,0.86]
Song Tianqiang 2021	11	42	17	44	6.1%	0.54 [0.25,1.43]
Zhang Zhihua 2014	3	46	5	46	2.3%	0.55 [0.11,2.53]
Xu Jiwei 2016	1	32	4	33	1.9%	0.22 [0.01,2.23]
Wang Zhu 2015	3	40	5	40	2.3%	0.55 [0.14,2.53]
Luo Hanchuan 2014	12	42	14	42	5.0%	0.82 [0.34,2.03]
Cai Lijun 2015	8	60	21	60	9.1%	0.27 [0.13,0.73]
Zhong Tiegang 2015	9	35	26	33	9.9%	0.07 [0.05,0.27]
Total (95% CI)		785		815	100.0%	0.63 [0.52,0.76]
Total events	264		353			

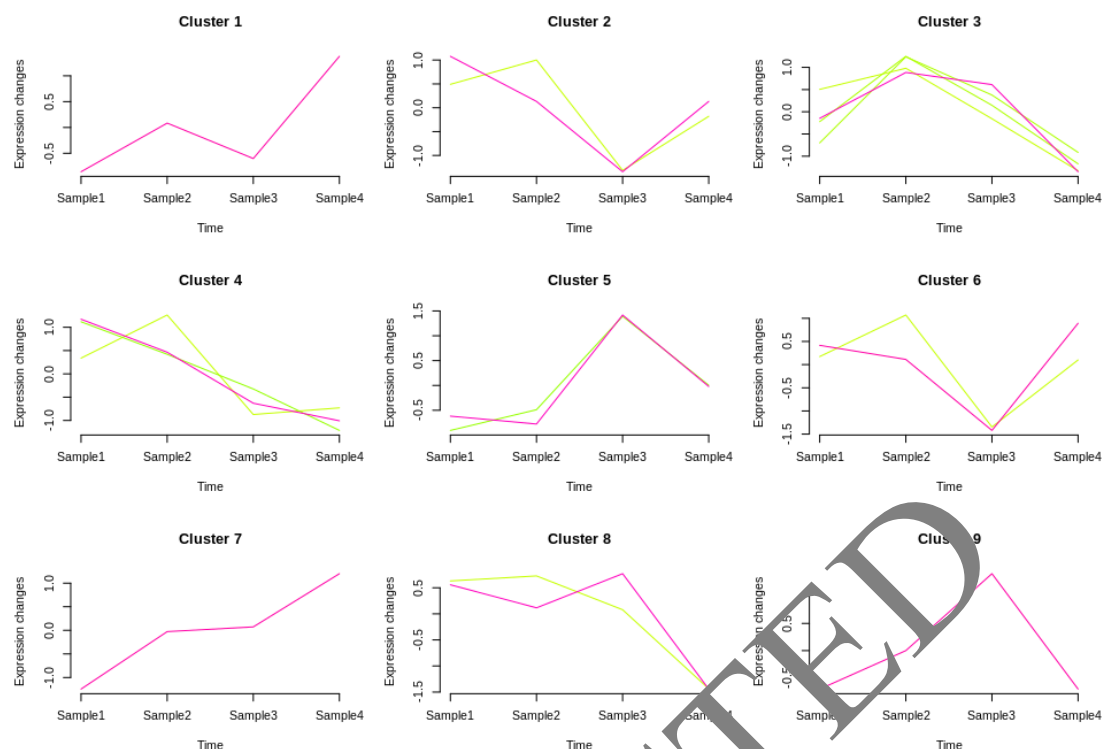


Figure 7. Comparison of positive resection margin (RM) rates between precision (ICG fluorescence imaging) and traditional approaches in laparoscopic liver resection for primary liver cancer.

Table 8. Comparison of 1-year SR between precision and traditional.

Study or Subgroup	Precision		General		Weight	Odds Ratio M-H, Fixed, 95%CI
	Events	Total	Events	Total		
Okamura 2014	12	139	68	97	18.6%	1.75 [0.99,3.26]
Sasaki 2013	25	30	45	57	6.5%	1.63 [0.31,3.44]
Tomimaru 2012	30	30	60	62	0.8%	2.53 [0.14,54.14]
Yamamoto 2017	80	125	36	4	19.4%	0.76 [0.34,1.54]
Song Tianqiang 2021	23	42	29	44	7.3%	1.92 [0.74,4.97]
Zhang Song 2015	120	158	24	49	10.6%	3.27 [1.67,6.44]
Zhang Lixian 2018	46	60	35	60	9.8%	2.33 [1.06,5.17]
Li Liuzheng 2019	66	101	50	101	20.8%	1.94 [1.07,3.37]
Wang Zhu 2015	38	40	36	40	2.2%	2.13 [0.35,12.26]
Luo Hanchuan 2014	37	42	26	33	4.2%	1.97 [0.55,6.99]
Total (95% CI)		767		591	100.0%	1.80 [1.37,2.36]
Total events	593		411			

There were 10 articles included to compare 1-year survival rate after surgery. Among number of cases, 767 cases were in precision and 591 cases were in traditional. The analysis results ($P = 0.36$, $I^2 = 9\%$) showed that there was homogeneity between outcome indicators. The OR was 1.80, 95%

CI (1.39,2.34) in Figure 8 and Table 8. The combined effect was $Z = 4.43$, $P < 0.0001$, survival rate after surgery was significant, the precision was higher.

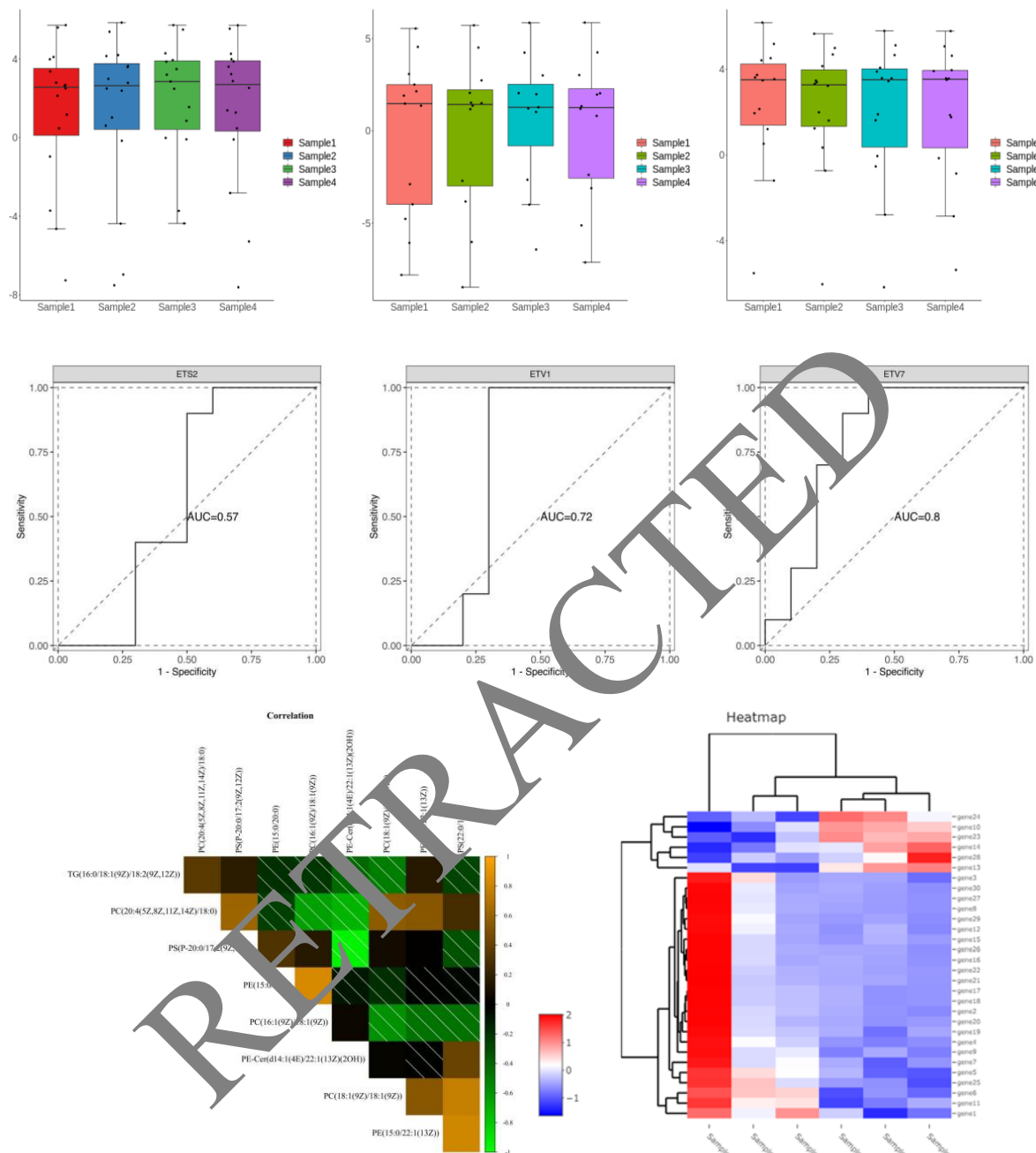


Figure 8. Comparison of 1-year survival rate (SR) between precision and traditional approaches in laparoscopic liver resection for primary liver cancer.

Publication bias was evaluated by making funnel plots. The incidence of postoperative complications and recurrence and metastasis rates were used for funnel plot analysis. It can be seen from Figures 9 and 10 that funnel plot experimental results were basically distributed on both sides of funnel plot, which was relatively symmetrical. The leaky funnel plots of other outcome indicators were also basically symmetrical, indicating that there was no obvious publication bias in this study; In addition, 33 articles included in this paper are of high-quality using Cochrane Reviewers' Handbook's

quality evaluation standard, which indicates that Meta analysis results have good authenticity.

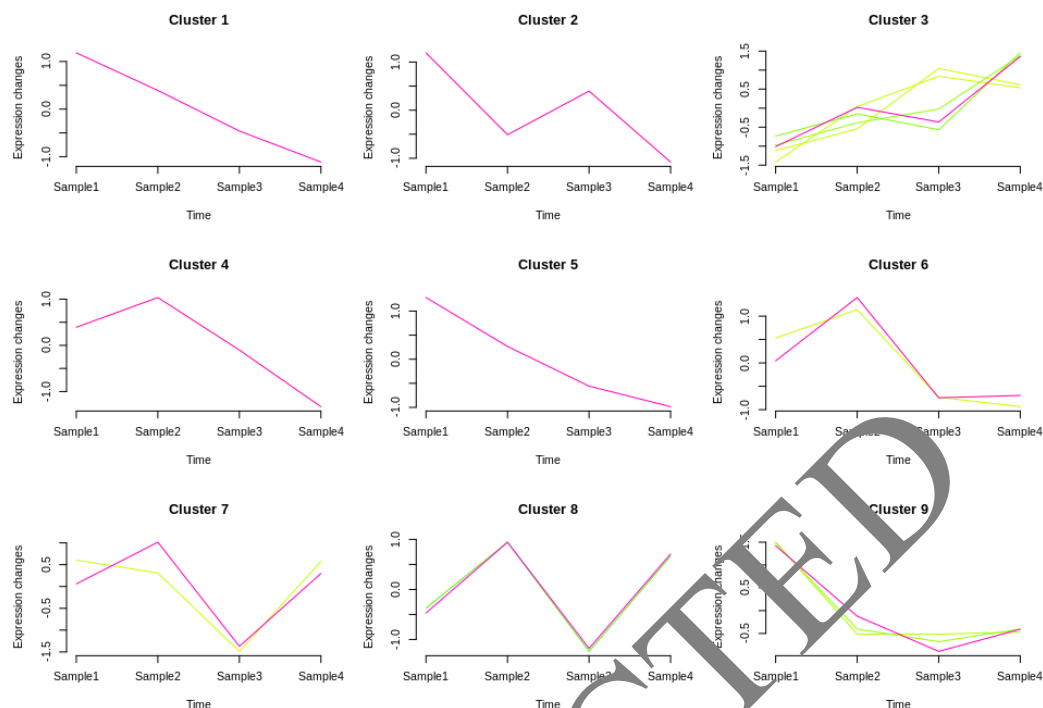
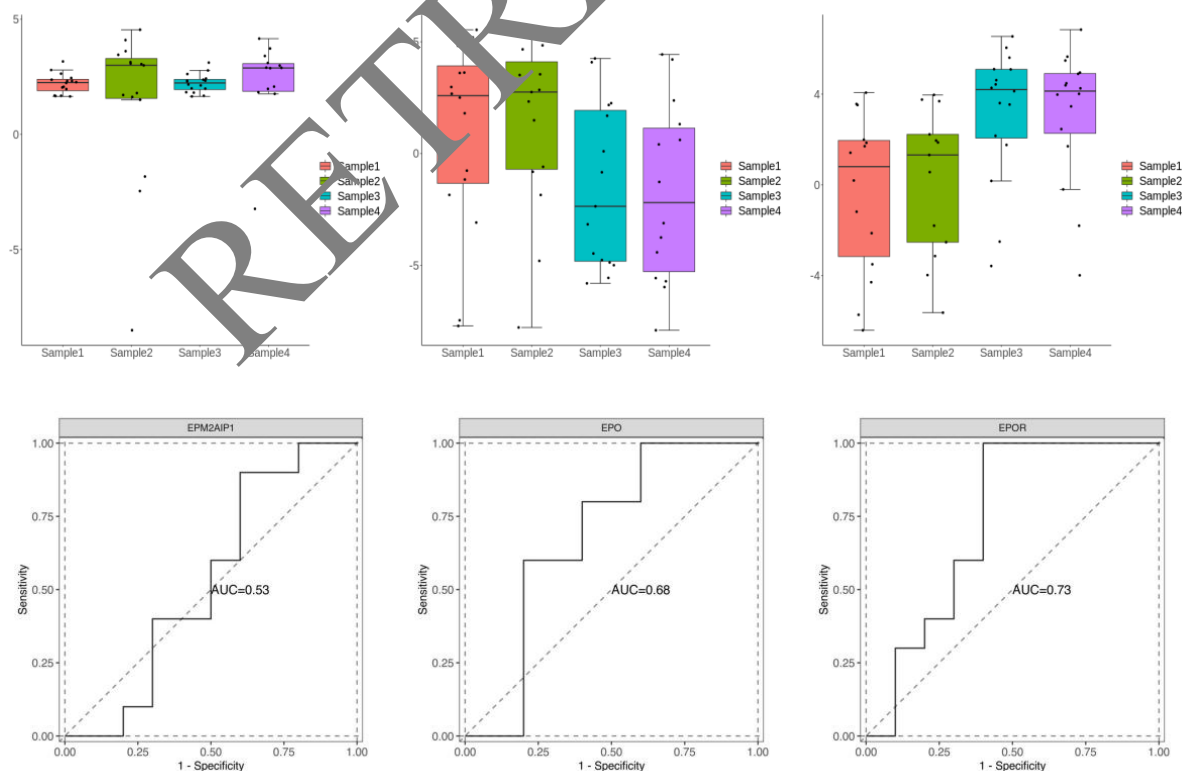


Figure 9. Funnel diagram of publication bias assessment for the positive conversion rate (PCR) in laparoscopic liver resection for primary liver cancer.



Continued on next page

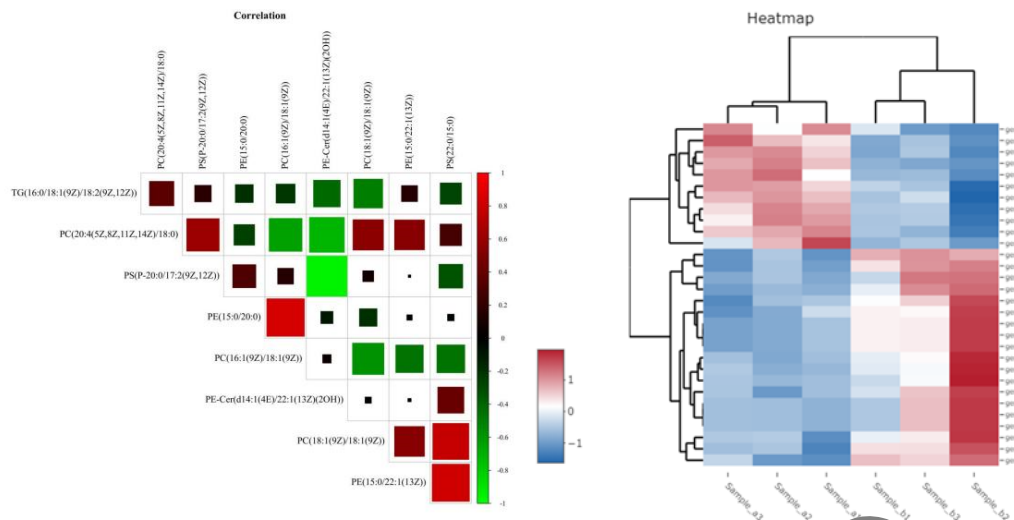


Figure 10. Funnel plot of publication bias assessment for recurrence and metastasis rates in laparoscopic liver resection for primary liver cancer.

4. Discussion

ICG fluorescence imaging is a valuable tool for laparoscopic liver resection in patients with primary liver cancer. It provides real-time visualization of liver blood supply, enabling surgeons to determine the best approach for liver resection and precise localization of the tumor. Moreover, ICG helps detect small liver tumors with greater accuracy, making the surgery more precise and significantly reducing the likelihood of complications; however, ICG application also has certain limitations. One of the major disadvantages is that the fluorescence signal may not be bright enough to visualize tumors owing to ICG clearance, which can cause dispersion. Moreover, although ICG helps in detecting tumors, it does not provide information about the tumor margin, which is crucial for complete tumor removal. ICG fluorescence imaging is a valuable clinical tool for laparoscopic resection of primary liver cancer. Despite some limitations, its clinical significance in enhancing the accuracy and precision of liver surgery cannot be underestimated.

The incidence of hepatocellular carcinoma in China has remained high in recent years. Early diagnosis and accurate radical treatment are crucial for determining the treatment effect and long-term prognosis. Progressive imaging technology has significantly improved tumor detection and resection rates during the clinical treatment of HCC. However, it remains challenging to identify and locate small lesions. With the widespread use of intraoperative ultrasound in clinical practice, the sensitivity and specificity of detecting sub-foci have improved, reducing missed diagnoses and misdiagnoses. It also accurately locates the tumor and identifies its adjacent relationship with the surrounding vascular system, making the tumor resection more thorough. However, intraoperative ultrasound is limited in detecting and differentiating small tumor lesions with a diameter of less than 1 cm, which makes it challenging to detect superficial lesions and provide real-time navigation for the operator during tumor resection. Therefore, there is a growing focus on tumor visualization technology in surgery, and the use of ICG as a medical imaging developer has been gaining popularity for more than 50 years. After ICG enters body via vein, it is quickly absorbed by liver cells to make liver appear fluorescence. After a few hours, it is almost completely excreted into biliary tract. Since it does not enter intestinal hepatic

circulation, liver fluorescence will gradually weaken and disappear. When liver cancer, liver cirrhosis nodules and inflammatory changes occur, ICG in focus remains and continues to show fluorescence compared with rapid excretion of surrounding normal liver tissue [26].

During laparoscopic liver resection for PLC, the amount of bleeding can decrease when using fluorescence-guided surgery with ICG fluorescence imaging technology [1–3]. There are several reasons for reduced bleeding, including improved visualization of the blood vessels. ICG fluorescence imaging allows surgeons to see blood vessels more clearly, minimizing the risk of unintentional injury or damage and reducing bleeding. Accurate identification of tumor boundaries is also possible with ICG fluorescence imaging, which can differentiate between tumor and normal liver tissue [3,4]. This precise delineation helps surgeons plan their resection strategy, accordingly, minimizing unnecessary resection of healthy tissue and reducing the risk of blood vessel injury. Finally, using ICG fluorescence imaging technology can lead to meticulous surgical planning and techniques. With real-time visual feedback, surgeons can guide their surgical approach carefully and precisely to dissect tissues and blood vessels. This increased attention to detail helps to minimize bleeding during the procedure [11–14]. When surgeons use ICG fluorescence imaging, they may be more cautious and meticulous in their surgical maneuvers. This is because imaging technology provides detailed information that can help to reduce bleeding. However, this heightened attentiveness and precision can also lead to a prolonged surgical time. This is because additional steps are required for imaging, identification and precise dissection of structures under fluorescence guidance. Nevertheless, surgeons may take more time to ensure accurate identification and safe resection of the tumor tissue while minimizing bleeding [15]. Although this extended surgical time can be considered a tradeoff for the benefits gained in improved surgical outcomes and reduced bleeding, it is essential to note that the exact reasons for reduced bleeding may vary between studies and individual cases [18–21].

ICG uptake by hepatocytes is achieved through two membrane transport systems (OATP1B3 transport carrier and NTCP transport polypeptide), while its excretion is achieved by MRP2 carrier system on hepatocyte membrane at side of bile capillaries. If the mechanism of some HCC cells to ingest ICG is normal and mechanism of excretion is impaired, residual ICG will cause HCC tumor substance to continue to show fluorescence [21,22]. Since it was reported that fluorescence imaging technology guided HCC tumor resection, more and more exploratory studies have been conducted in field of liver surgery to guide surgeons to make surgical decisions. When ICG cannot be excreted through the hepatobiliary system after ingestion by the lesion, resulting in sustained fluorescence at the target site, it is important to identify a solution to address the inability of the lesion to ingest drugs or sensors at the onset stage. Approaches that could be explored include the use of alternative imaging agents, co-administration of enhancing agents, developing targeted delivery systems and performing a sensitivity analysis. Tailored strategies can be developed by identifying the underlying factors contributing to the ingestion issue [1–6,15–18].

Based on the analysis of the study, it was found that all outcome indicators of precision and traditional were significant. It was observed that precision has a longer operation time than traditional, while other indicators are better and hospital stay is slightly different [23]. After carefully reading the included literature, the reasons for these results were analyzed in detail. It was found that preoperative evaluation of the patient's liver function is emphasized by PH, along with the use of sophisticated surgical operations and 3D imaging technology to increase preoperative preparation time. During the operation, a careful search for the cut edge was carried out, accurate liver parenchyma disconnection was implemented, and new instruments were used along with the measurement of residual liver volume.

The edge of the liver to be cut was carefully separated, and these meticulous operations extended the operation time. However, they also help to reduce intraoperative bleeding and the risk of surgery. Patients with liver cancer often suffer from liver dysfunction, which makes it crucial to apply an individualized principle to different patients before hepatectomy, calculate the residual liver volume and thoroughly evaluate residual liver function. This approach can help reduce the residual liver volume and minimize the chances of liver dysfunction after surgery [24]. It is very important to report residual liver volume, which is closely related to serious postoperative complications. When residual liver volume is less than 25%, incidence of complications is increased [25]. It is also confirmed that residual liver volume is closely related to postoperative liver failure and is an important factor. Moreover, due to the large number of hepatitis B patients in China, there are many patients with hepatitis B cirrhosis. Therefore, it is particularly important to calculate amount of residual liver and evaluate function of residual liver. Following the concept of accurate hepatectomy, it has advantages in postoperative liver function indicators and complication rate. PH is to maximize protection of functional liver parenchyma on premise of ensuring thorough removal of target lesions, maximize surgical benefits with minimal surgical invasion, improve 1-year survival rate of patients after surgery and promote early and rapid recovery of patients.

When it comes to fluorescence guidance during surgery, it is crucial to consider some possible factors that can contribute to an extended surgical time. One such factor is the technical consideration involved. Fluorescence-guided surgery requires additional steps, such as administration of the fluorescent dye and calibration of the imaging system, which can add to the overall surgical time. Additionally, complex tumor characteristics, such as irregular shapes, can prolong surgery since delicate dissection is required to ensure complete resection while preserving the surrounding healthy tissue. Surgeons' experience with the technique can also play a role, as surgeons new to using ICG fluorescence imaging may require more time to familiarize themselves with the technique. Finally, intraoperative decisions made by the surgeon, such as adjusting the surgical plan to optimize the outcome, can also contribute to extended surgical time. The impact on surgical time can vary depending on several factors, including surgeon expertise and patient characteristics.

There are various explanations for the decreased recurrence rate observed in the context of fluorescence-guided surgery using ICG fluorescence imaging technology in laparoscopic liver resection for PLC [7–10]. One of the reasons for this could be the enhanced visualization of tumor boundaries and the ability to identify and delineate tumor tissue during surgery accurately. This can help surgeons achieve complete resection and reduce the likelihood of residual tumor cells and subsequent recurrence [11]. Additionally, fluorescence imaging technology can contribute to a decrease in positive margin rates, leading to a lower recurrence rate. Moreover, it can aid in accurately identifying and localizing lesions associated with PLC, allowing surgeons to perform complete resections and reduce the risk of recurrence [11,15]. However, it is important to note that different tumor types and anatomical considerations can influence the efficacy of fluorescence-guided surgical techniques [1–6]. Therefore, each specific context and tumor type requires an independent evaluation.

This study has the following shortcomings: ① In this study, some of included literature may be due to characteristics of patients' cases, and it is necessary to select an appropriate surgical scheme according to the condition of the patient. It is impossible to carry out a complete random allocation and blind method, which has a certain impact on quality evaluation of literature; ② Although patients can tolerate surgery, whether a patient has other basic diseases or not is not described in some literatures; ③ The English literature included in this study is less representative, and only outcome

indicators of short-term efficacy are analyzed. Therefore, we look forward to a higher quality long-term follow-up study to evaluate the application of the concept of PH.

Data Availability

The experimental data used to support the findings of this study are available from the corresponding author upon request.

Use of AI tools declaration

The authors declare they have not used Artificial Intelligence (AI) tools in the creation of this article.

Conflicts of interest

The authors declared that they have no conflicts of interest regarding this work.

References

1. R. Souzaki, N. Kawakubo, T. Matsuura, K. Yoshimatsu, Y. Koga, J. Takemoto, et al., Navigation surgery using indocyanine green fluorescent imaging for hepatoblastoma patients, *Pediatr. Surg. Int.*, **35** (2019), 551–557. <https://doi.org/10.1007/s00383-019-04458-5>
2. R. S. Whitlock, K. R. Patel, T. Yang, H. N. Nguyen, P. Masand, S. A. Vasudevan, Pathologic correlation with near infrared-indocyanine green guided surgery for pediatric liver cancer, *J. Pediatr. Surg.*, **57** (2022), 700–710. <https://doi.org/10.1016/j.jpedsurg.2021.04.019>
3. P. He, T. Huang, C. Fang, S. Su, T. Tian, X. Xia, et al., Identification of extrahepatic metastasis of hepatocellular carcinoma using indocyanine green fluorescence imaging, *Photodiagn. Photodyn. Ther.*, **25** (2019), 417–420. <https://doi.org/10.1016/j.pdpdt.2019.01.031>
4. G. Piccolo, M. Barabino, M. Diano, E. Lo Menzo, A. G. Epifani, F. Lecchi, et al., Application of indocyanine green fluorescence as an adjuvant to laparoscopic ultrasound in minimally invasive liver resection, *J. Laparoendosc. Adv. Surg. Tech.*, **31** (2021), 517–523. <https://doi.org/10.1089/lap.2020.0895>
5. E. Lieto, G. Garzía, F. Cardella, A. Mabilia, N. Basile, P. Castellano, et al., Indocyanine green fluorescence imaging-guided surgery in primary and metastatic liver tumors, *Surg. Innovation*, **25** (2018), 62–68. <https://doi.org/10.1177/1553350617751451>
6. Y. Xu, M. Chen, X. Meng, P. Lu, X. Wang, W. Zhang, et al., Laparoscopic anatomical liver resection guided by real-time indocyanine green fluorescence imaging: experience and lessons learned from the initial series in a single center, *Surg. Endoscopy*, **34** (2020), 4683–4691. <https://doi.org/10.1007/s00464-020-07691-5>
7. Y. Miyazaki, M. Kurata, Y. Oshiro, O. Shimomura, K. Takahashi, T. Oda, et al., Indocyanine green fluorescence-navigated laparoscopic metastasectomy for peritoneal metastasis of hepatocellular carcinoma: a case report, *Surg. Case Rep.*, **4** (2018), 1–4. <https://doi.org/10.1186/s40792-018-0537-x>

8. E. Kose, B. Kahramangil, H. Aydin, M. Donmez, H. Takahashi, L. A. Acevedo-Moreno, et al., A comparison of indocyanine green fluorescence and laparoscopic ultrasound for detection of liver tumors, *HPB*, **22** (2020), 764–769. <https://doi.org/10.1016/j.hpb.2019.10.005>
9. K. Yamamura, T. Beppu, N. Sato, K. Kinoshita, E. Oda, H. Yuki, et al., Complete removal of adrenal metastasis in hepatocellular carcinoma using indocyanine green fluorescent imaging, *Anticancer Res.*, **40** (2020), 5823–5828. <https://doi.org/10.21873/anticancer.14600>
10. M. Franz, J. Arend, S. Wolff, A. Perrakis, M. Rahimli, V. R. Negrini, et al., Tumor visualization and fluorescence angiography with indocyanine green (ICG) in laparoscopic and robotic hepatobiliary surgery—valuation of early adopters from Germany, *Innovative surgical sciences*, **6** (2021), 59–66. <https://doi.org/10.1515/iss-2020-0019>
11. T. Aoki, M. Murakami, T. Koizumi, K. Matsuda, A. Fujimori, T. Kusano, et al., Determination of the surgical margin in laparoscopic liver resections using infrared indocyanine green fluorescence, *Langenbecks Arch. Surg.*, **403** (2018), 671–680. <https://doi.org/10.1007/s00423-018-1685-y>
12. H. Lu, J. Gu, X. F. Qian, X. Z. Dai, Indocyanine green fluorescence navigation in laparoscopic hepatectomy: a retrospective single-center study of 120 cases, *Surg. Today*, **51** (2021), 695–702. <https://doi.org/10.1007/s00595-020-02163-8>
13. T. Urade, H. Sawa, Y. Iwatani, T. Abe, R. Fujinaka, K. Murata, et al., Laparoscopic anatomical liver resection using indocyanine green fluorescence imaging, *Asian J. Surg.*, **43** (2020), 362–368. <https://doi.org/10.1016/j.asjsur.2019.04.008>
14. T. Aoki, T. Koizumi, D. A. Mansour, A. Fujimori, T. Kusano, K. Matsuda, et al., Ultrasound-guided preoperative positive percutaneous indocyanine green fluorescence staining for laparoscopic anatomical liver resection, *J. Am. Coll. Surg.*, **230** (2020), e7–e12. <https://doi.org/10.1016/j.jamcollsurg.2019.11.004>
15. M. V. Marino, S. Di Saverio, M. Podda, M. Gomez Ruiz, M. Gomez Fleitas, The application of indocyanine green fluorescence imaging during robotic liver resection: a case-matched study, *World J. Surg.*, **43** (2019), 2555–2606. <https://doi.org/10.1007/s00268-019-05055-2>
16. H. Zou, X. Yang, Q. L. Li, Q. X. Zhou, L. Xiong, Y. Wen, A comparative study of albumin-bilirubin score with Child-Pugh score, model for end-stage liver disease score and indocyanine green R15 in predicting posthepatectomy liver failure for hepatocellular carcinoma patients, *Dig. Dis.*, **36** (2021), 235–243. <https://doi.org/10.1159/000486590>
17. K. Purich, J. P. Dang, A. Poonja, W. Y. Sun, D. Bigam, D. Birch, et al., Intraoperative fluorescence imaging with indocyanine green in hepatic resection for malignancy: a systematic review and meta-analysis of diagnostic test accuracy studies, *Surg. Endoscopy*, **34** (2020), 2891–2903. <https://doi.org/10.1007/s00464-020-07543-2>
18. G. Piccolo, M. Barabino, A. Pesce, M. Diana, F. Lecchi, R. Santambrogio, et al., Role of indocyanine green fluorescence imaging in minimally invasive resection of colorectal liver metastases, *Surg. Laparoscopy Endoscopy Percutaneous Tech.*, **32** (2022), 259–265. <https://doi.org/10.1097/SLE.0000000000001037>
19. J. Zhou, J. Sun, W. Zhang, Z. Lin, Multi-view underwater image enhancement method via embedded fusion mechanism, *Eng. Appl. Artif. Intell.*, **121** (2023), 105946. <https://doi.org/10.1016/j.engappai.2023.105946>

20. D. K. Kim, J. I. Choi, M. H. Choi, M. Y. Park, Y. J. Lee, S. E. Rha, et al., Prediction of posthepatectomy liver failure: MRI with hepatocyte-specific contrast agent versus indocyanine green clearance test, *Am. J. Roentgenol.*, **211** (2018), 580–587. <https://doi.org/10.2214/AJR.17.19206>
21. J. L. Petrick, K. A. McGlynn, The changing epidemiology of primary liver cancer, *Curr. Epidemiol. Rep.*, **6** (2019), 104–111. <https://doi.org/10.1007/s40471-019-00188-3>
22. Z. Liu, Y. Jiang, H. Yuan, Q. Fang, N. Cai, C. Suo, et al., The trends in incidence of primary liver cancer caused by specific etiologies: results from the Global Burden of Disease Study 2016 and implications for liver cancer prevention, *J. Hepatol.*, **70** (2019), 674–683. <https://doi.org/10.1016/j.jhep.2018.12.001>
23. J. Zhou, H. C. Sun, Z. Wang, W. M. Cong, J. H. Wang, M. S. Zeng, et al., Guidelines for diagnosis and treatment of primary liver cancer in China (2017 Edition), *Liver Cancer*, **7** (2018), 235–260. <https://doi.org/10.1159/000488035>
24. M. Kudo, K. H. Han, S. L. Ye, J. Zhou, Y. H. Huang, S. M. Lin, et al., A changing paradigm for the treatment of intermediate-stage hepatocellular carcinoma: Asia-Pacific primary liver cancer expert consensus statements, *Liver Cancer*, **9** (2020), 245–260. <https://doi.org/10.1159/000507370>
25. Y. X. Gao, T. W. Yang, J. M. Yin, P. X. Yang, B. X. You, M. Y. Chai, et al., Progress and prospects of biomarkers in primary liver cancer, *Int. J. Oncol.*, **57** (2020), 54–66. <https://doi.org/10.3892/ijo.2020.5035>
26. R. Sharma, Descriptive epidemiology of incidence and mortality of primary liver cancer in 185 countries: evidence from GLOBOCAN 2018, *Jpn. J. Clin. Oncol.*, **50** (2020), 1370–1379. <https://doi.org/10.1093/jjco/hyaa130>



AIMS Press

©2023 the Author(s), licensee AIMS Press. This is an open access article distributed under the terms of the Creative Commons Attribution License (<http://creativecommons.org/licenses/by/4.0>)